Comparison of the results from (D5a) and (D5b) gave an idea of the accuracy with which we had calculated the integrand. Agreement was found to be better than 1%.

The results plotted in Fig. 7 (integration over $\sigma$ and $\chi$) were obtained from the results shown in Figs. 5 and 6 by noting that the $p_T$ distribution for $\chi=\frac{1}{4}\pi$ is not far different from what would have been predicted from the distribution for $\chi=\frac{1}{2}\pi$ assuming isotropy. Curves for $=\chi\ \frac{1}{12}\pi, \frac{1}{6}\pi, \frac{1}{3}\pi, (5/12)\pi$ were plotted using this fact and the calculated distributions for $\chi=\frac{1}{4}\pi$ and $\frac{1}{2}\pi$ and then the integration performed numerically from the graph. Errors involved in this procedure are negligible compared to other approximations already made.

PHYSICAL REVIEW VOLUME 129, NUMBER 2 15 JANUARY 1963

# Production of Tritons, Deuterons, Nucleons, and Mesons by 30-GeV Protons on Al, Be, and Fe Targets*

A. SCHWARZSCHILD AND Č. ZUPANČIČ†
*Brookhaven National Laboratory, Upton, New York*
(Received 2 August 1962)

The momentum spectra of particles emerging at 30° to a 30-GeV proton beam impinging upon various targets were measured using time-of-flight techniques. Intensities of protons, antiprotons, $\pi$ mesons, $K$ mesons, deuterons, and tritons in the range 1 to 3 GeV/$c$ are given. Particular attention is given to the tritons and deuterons emitted from the different targets. Possible mechanisms for their production are discussed.

## I. INTRODUCTION

DURING the initial investigations of the composition of secondary particle beams emitted at various angles from internal targets in the 33-GeV alternating gradient synchrotron (AGS) at Brookhaven National Laboratory, we analyzed the beam emerging at 30° by measuring the time of flight of particles after momentum selection by magnetic deflection. The results of the beam surveys at other angles were performed by other groups and have been reported.[1,2] Our results on the intensities of emerging beams of pions, protons, antiprotons, and $K$ mesons are presented mainly for the practical interest in these investigations for the design of future experiments at the AGS.

The copious production of deuterons and mass-three nuclei, discovered at CERN[3] during the observation of forward secondary beams, was also observed at 30° with very little change in intensity relative to pions and protons. If these particles were produced in nucleon-nucleon collisions, one would expect, on the basis of kinematical arguments, that their yield would decrease rapidly at the larger laboratory angles. The large observed yield suggests strongly that the production of these particles involves cooperative phenomena involving several nucleons of the target nucleus. We have studied the momentum distributions from ~1 to 3 GeV/$c$ of these particles (at 30°) from various target nuclei. The main subject of this paper is a report of these measurements and a discussion of the results in terms of existing models.

## II. EXPERIMENTAL TECHNIQUE AND RESULTS

### 1. Counter Arrangements and Electronics

A schematic diagram of the beam layout is given in Fig. 1. The beam of secondary particles emerging from the internal target at 30° from the AGS beam passed through a hole (~6-in.×8-in. cross section) in the main machine shielding wall. Thirty-eight feet from the target the beam passed through a lead collimator 30 in. long with a 1 in. wide and 2 in. high aperture. A 35-in. variable field magnet immediately following the collimator analyzed the particles with respect to their momentum. The two scintillation counters used to determine the time of flight were placed on a line making an 8° angle with the collimated beam. The back counter position was fixed at ~33 ft from the center of the bending magnet. The forward counter position was varied from 6 to 20 ft from the back counter according to the desired resolution.

The first scintillator was $\frac{1}{2}$ in.×$\frac{1}{2}$ in.×$\frac{1}{4}$ in. Pilot B mounted directly on one of its smaller surfaces to an Amperex 56 AVP photomultiplier placed perpendicular

* Work performed under the auspices of the U. S. Atomic Energy Commission.
† On leave from the University of Ljubljana, Ljubljana, Yugoslavia.
[1] W. F. Baker, R. L. Cool, E. W. Jenkins, T. F. Kycia, S. J. Lindenbaum, W. A. Love, D. Luers, J. A. Niederer, S. Ozaki, A. L. Read, J. J. Russell, and L. C. L. Yuan, Phys. Rev. Letters 7, 101 (1961).
[2] V. L. Fitch, S. L Meyer, and P. A. Piroue, Phys. Rev. 126, 1849 (1962).
[3] V. T. Cocconi, T. Fazzini, C. Fidecaro, M. Legros, N. H. Lipman, and A. W. Merrison, Phys. Rev. Letters 5, 19 (1960); L. Gilly, B. Leontic, A. Lundby, R. Meunier, J. P. Stroot, and M. Szeptycka, *Proceedings of the 1960 Conference on High-Energy Physics at Rochester*, (Interscience Publishers, Inc., New York, 1960).

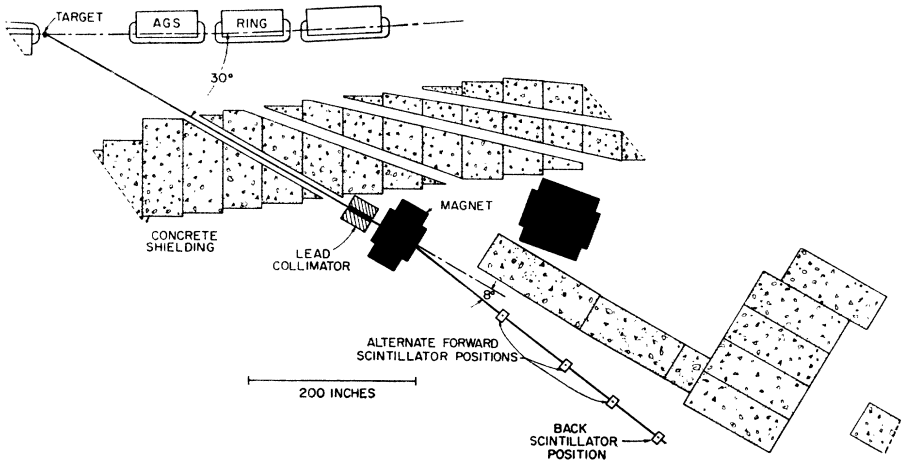


FIG. 1. Experimental arrangement.

to the beam. The back scintillator was a $1\frac{1}{2}$-in diam.$\times$2-in.-long plastic viewed directly through the flat surface by a 56 AVP multiplier. The beam passed down the axis of this second multiplier. (No spurious pulses seemed to arise from direct interaction of the beam with the multiplier structure.) In the geometry the effective solid angle and momentum resolution is determined by the collimator and both scintillators, but it is still easily calculable.

The electronic system incorporated a conventional 6BN6 time to amplitude converter which was operated by pulses derived from a Western Electric 404A limiter driven to cutoff by the photomultiplier plate pulses. Some pulse-height selection was employed to obtain optimum-time resolution. The time spectra were displayed on an RIDL 400-channel analyzer. The memory of this analyzer can be split into 4 groups by gating pulses. A schematic of the electronics employed and some special techniques used to improve time resolution, prevent pile-up, and simultaneously perform $dE/dx$ measurements are described in the Appendix.

During the course of these experiments the energy of the primary AGS beam was varied between 28 and 33 GeV. These variations, required by other simultaneous experiments, were beyond our control. However, very little difference in relative yields of different particles at a fixed outgoing momentum was observed and no attempt was made to correct for these effects. The beam survey data were all performed at 29.5 GeV. The AGS beam was operated at all times for counter groups and attempts were made to obtain long spills of the beam on the target. Total circulating beams of the order of $3\times10^{10}$ particles per burst were spilled on the target over a period of between 50 and 150 msec. Our geometric efficiency was sufficiently poor so that pile-up and accidental rates were negligible. Typical singles rates on the forward detector were several thousand per beam pulse and coincidence rates of the order of 200 counts per beam pulse were recorded in the low momentum runs. Thus, the relatively long pulse-height analyzer dead time ($\sim$50 $\mu$sec) did not seriously affect the counting efficiency. All data presented, however, have been corrected for analyzer dead time effects.

Two typical time spectra are shown in Figs. 2 and 3 for illustrative purposes. Figure 2 shows a spectrum taken to determine $K^+$ intensities. The split memory was utilized in order to restrict the range of acceptable pulse heights. The solid points correspond to pulses in both scintillators having amplitudes which lie between the maxima of the Landau distribution for $\pi^+$ and protons. The open circled curve (taken simultaneously) contains a time spectrum of all other amplitude pulse pairs. The improved time resolution, the improved peak-to-valley ratio, and the emphasis of $\pi^+$ to proton peak heights

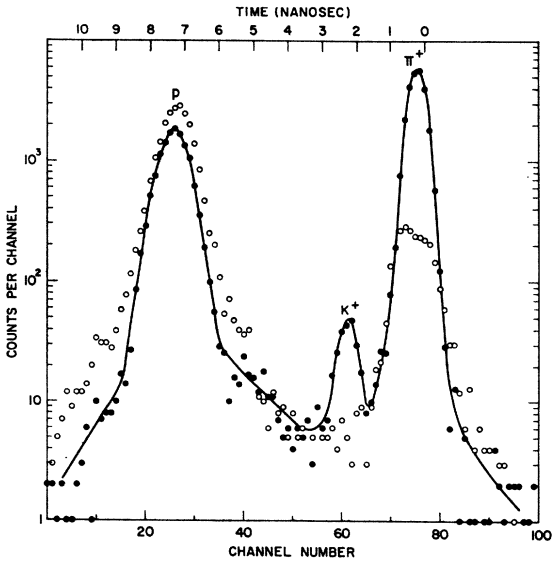


FIG. 2. Time-of-flight spectra obtained at 1 GeV/$c$ with a counter separation of 20 ft. The two curves are described in the test. The target was carbon.

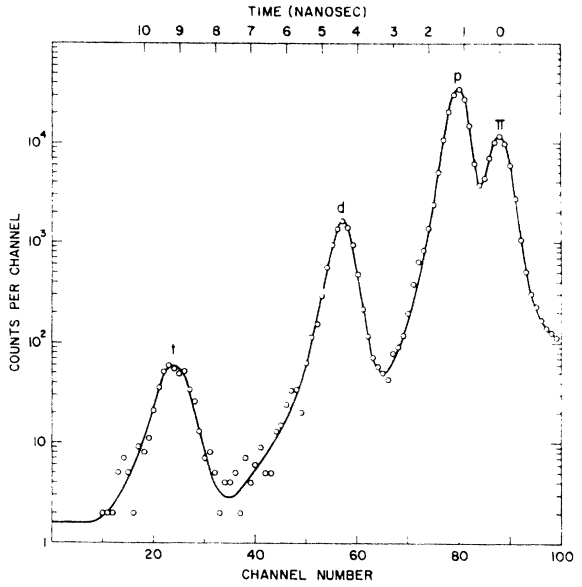


FIG. 3. Time-of-flight spectrum obtained at 2 GeV/$c$ with a counter separation of 12 ft. The target was aluminum.

are all consistent with the pulse-height requirements. The advantage of the use of the split memory arrangement is the improved resolution in the "channeled" curve along with the preservation of proper total intensities when both curves are added together. Figure 3 shows a typical time spectrum obtained at higher momentum and smaller counter spacing for the determination of $d$ and $t$ intensities. These curves were taken with no restriction on energy loss in the scintillators, except that the multiplier output pulses were required to be larger than several times the noise level.

## 2. Beam Monitoring

For the purpose of obtaining absolute yields of particles and also proper relative yields for different particles at different momenta, monitoring of the internal beam is required. An induction-type beam monitor exists to measure the total circulating beam in the AGS. With moderately thin targets ($\sim$1 g/cm$^2$) multiple traversals occur until about 25 to 50% of the complete circulating beam of the AGS is lost by nuclear interactions in the target. Since this fraction was not accurately known, our absolute-yield measurements are given per circulating proton. This fraction also varied with exact machine parameters. The target efficiency was observed to change by about a factor of 2 during the runs. A separate counter monitor placed between the lead collimator, and the entrance to the deflecting magnet was used to normalize runs taken at different magnetic fields, and this was calibrated to within a factor of 2 with the circulating beam monitor to obtain absolute intensities.

## 3. Scattering Corrections and Absolute Yields

The absolute number of particles detected, as well as the ratios of different mass particles at various momenta, may be seriously affected by differences in multiple scattering in the forward counter, by absorption and by small counter misalignment. A calculation of corrections for these effects is extremely complicated with our experimental arrangement. Rather than try to correct theoretically for multiple scattering, we took data at several distances between the telescope counters and corrected for the scattering by extrapolation to zero separation of the counters. Absorption was small in most cases. Care was taken in aligning the telescope with the use of standard surveying techniques. Nevertheless, we feel that systematic errors could be considerable, perhaps as large as 30% for the heavier particles.

Figure 4 shows the momentum spectrum of the total number of all particles, irrespective of mass, detected with three different distances (6 ft, 12 ft, and 20 ft) between the first and second counter. For these runs the second counter (furthest from magnet) was left fixed, and the forward counter position was varied. The absolute intensity for each position was calculated (relative to the machine monitor) to include only the geometric efficiency but not the scattering corrections. The effect of scattering at large distance between the counters, and at low momentum, is clear. It is assumed that the solid curve, drawn as the envelope of the individual runs, is a relatively true picture of the momentum distribution corrected for scattering effects.

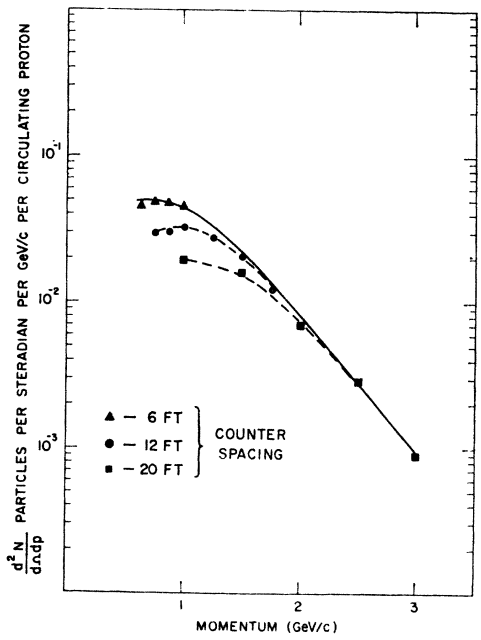


FIG. 4. Yield of all particles (uncorrected for decay) from a carbon target. The data were taken with 6 ft, 12 ft, and 20 ft between the two counters. These points are not corrected for scattering.

A similar procedure was used to correct the spectra for each of the individual particle yields.

Figure 5 shows the result of the survey for all the masses studied. Errors shown on this plot are purely statistical (counting errors). The statistical error on the $\pi$, $p$, $d$, and $t$ yields are quite small and are not shown. It is estimated that the error due to monitoring, target efficiency, and multiple scattering may be as large as a factor of 2 at any point on these curves.

### 4. Relative Yields of Particles from Aluminum Target

The relative yields obtained from an Al target are shown in Figs. 6 and 7. Since all particles at a given momentum are detected "simultaneously" with the time-analyzer method, these curves can be obtained independently of any knowledge of absolute machine intensity or target efficiency. The only corrections made to the raw data are for variations of scattering loss with mass at a particular momentum. These were performed on the basis of the empirical data obtained from the varying counter distance experiments. The errors shown in the figures are purely statistical. Errors due to uncertainties in scattering corrections are probably less than 30%.

### 5. Variation of Particles Ratios with Target $Z$

The data presented in this section were obtained with the use of an alternating target arrangement. On alternate beam pulses of the AGS, targets consisting of either Be or Al were flipped into the 30-GeV proton beam. The time spectra were stored alternately in two sections of the RIDL pulse-height analyzer. In this way mass spectra were accumulated at various momenta. The results of these experiments are presented in Fig. 8. Since all the geometric conditions are identical for both targets (except for an insignificant slight displacement in the target position), these data, as presented, are not subject to any scattering corrections. Neither are the data dependent upon target efficiency. The errors shown in the figures are purely statistical counting errors, and possible systematic errors should be negligible.

For several hours of running time alternating stainless steel and aluminum targets were used. Similar

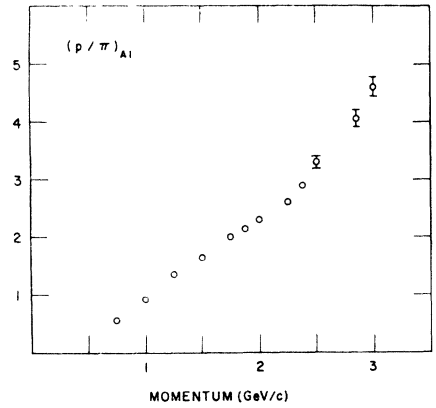


FIG. 6. Relative yields of proton to pion as a function of momentum, observed from an aluminum target. The pion yield has been corrected for decay and it was assumed that the pion beam is not contaminated by $e+\mu$.

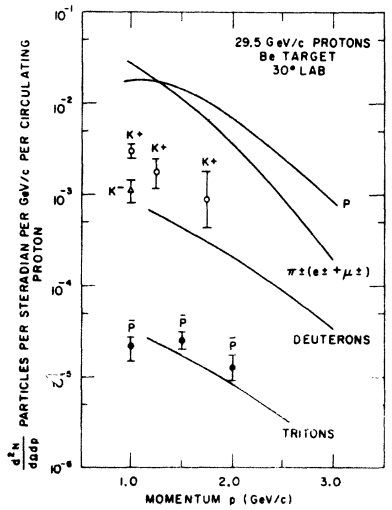


FIG. 5. Momentum distribution of particles observed. The data for $K$ and $\pi$ have been corrected for decay back to the target position. The $\pi$-decay correction assumes that there is negligible $\mu+e$ contamination. The data were corrected for scattering in counters as described in the text.

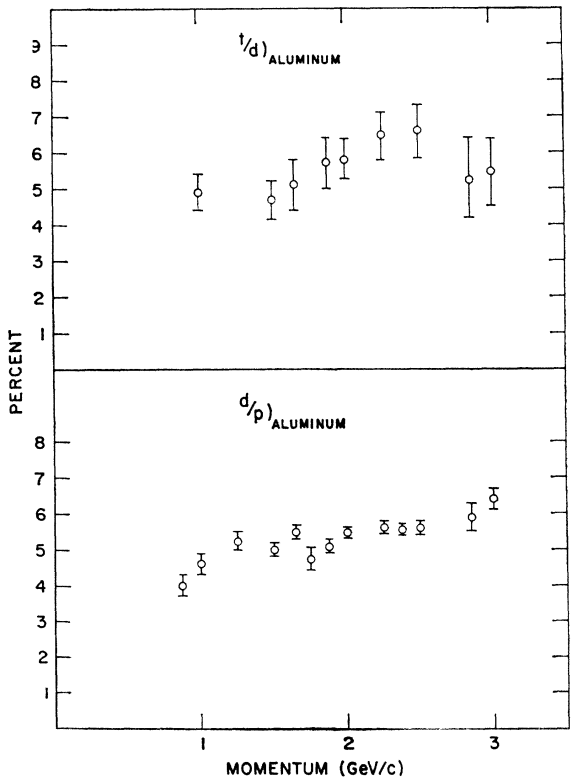


FIG. 7. Triton-to-deuteron, and deuteron-to-proton ratios as function of momentum for aluminum target.

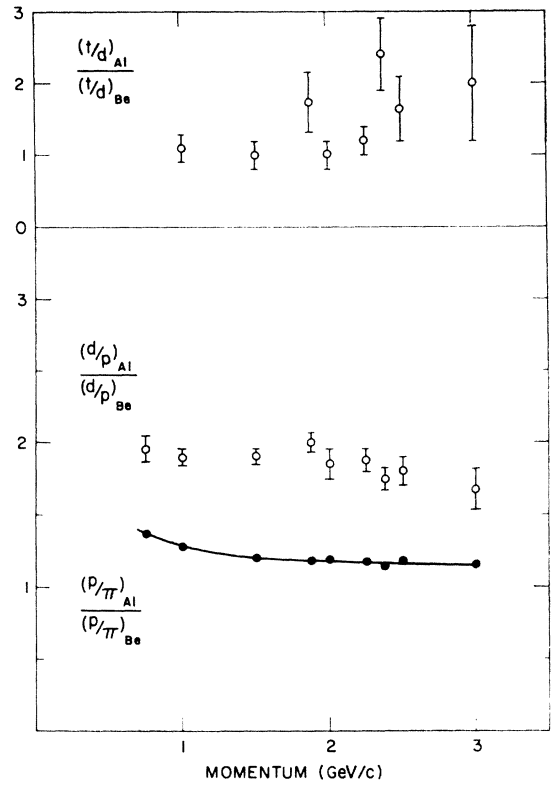


FIG. 8. Comparison of relative yields from aluminum and beryllium targets.

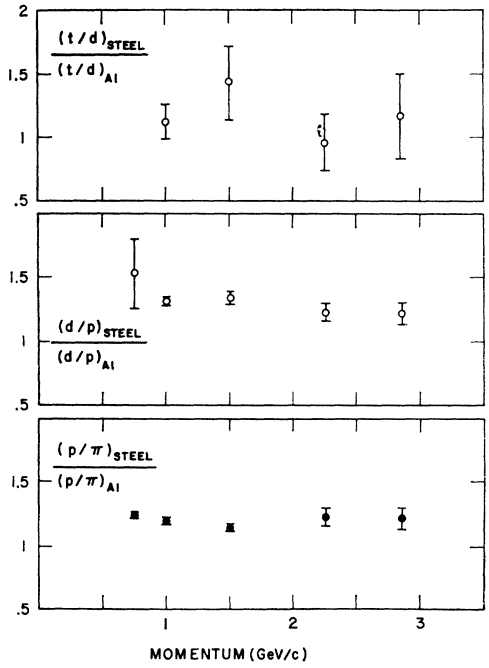


FIG. 9. Comparison of relative yields from steel and aluminum targets.

ratios to those shown comparing Be and Al are given for steel and Al in Fig. 9.

## III. DISCUSSION

### 1. Elementary Particles

At 30° in the laboratory the antiprotons are relatively less abundant than at smaller angles. The spectra of other elementary particles, pions, $K$ mesons and protons show the same general trend as at more forward angles. The pion spectrum fits into a picture, discussed by Cool,[4] of production in elementary nucleon-nucleon collisions. Transforming all pion spectra measured at different angles into the c.m. system of the incoming proton and a nucleon at rest, Cool obtains approximate symmetry around 90° and strong forward-backward peaking. The average transverse momentum is approximately 0.3 GeV/$c$.

The proton spectra measured at 30° and at more forward angles can be represented by an empirical expression, which fits the experimental results to within a factor of 2. The number of protons at laboratory momentum $k$ and angle $\theta$ is given by

$$dN_p(k)=2\times10^{-2}\frac{e^{-[(k\theta)^2/0.7]}}{k\sin\theta}\frac{k^2dkd\Omega}{E}$$

per circulating proton, (1)

energy $E$ being measured in units of GeV, momentum $k$ in GeV/$c$, and solid angle in steradians. Apart from the invariant phase space factor $k^2dkd\Omega/E$, the expression depends essentially only on the transverse momentum $k\sin\theta\approx k\theta$. That means that by transforming into the c.m. system of a nucleon-nucleon collision one would again obtain symmetry around 90° and strong forward-backward peaking. The average transverse momentum of protons is about 0.4 GeV/$c$, i.e., substantially larger than that of pions. However, the dependence of the proton-to-pion ratio on the target element indicates that nuclear effects must influence the production of at least one of them. Also, the proton spectra at angles larger than 30° are not fitted by the above expression, indicating perhaps a change in the physical process giving rise to those protons.

### 2. Deuterons and Tritons

The discovery of large numbers of deuterons and mass-three nuclei in secondary beams at the 28-GeV proton synchrotron at CERN came first as a surprise but the order of magnitude of the effect was soon explained by Hagedorn[5] on the basis of the statistical

[4] R. L. Cool, *Proceedings of the International Conference on High-Energy Accelerators, 1961* (U. S. Government Printing Office, Washington 25, D. C., 1961).

[5] R. Hagedorn, Phys. Rev. Letters 5, 276 (1960).

theory. Hagedorn's calculations cannot be directly applied to our measurements since he assumed that deuterons are produced in elementary collisions of incident protons with nucleons. Our laboratory angle of 30° is just beyond the kinematical limit for such deuterons. If one tried to argue that they might be produced in elementary collisions with nucleons in Fermi motion or slightly scattered out of their original direction, one should at least expect a spectrum shape with a peak around 3 GeV/$c$ which is the momentum of such dueterons at the limiting angle. The experiments clearly do not exhibit such peaking. The strong dependence of the deuteron-to-proton ratio on the target element is a further indication of the nuclear origin of the deuterons observed at 30°.

A simple mechanism for production of deuterons in nuclei would be a two-step process with the incident proton creating a shower in the nucleus and secondary nucleons giving rise to deuterons during their subsequent collisions with nucleons in the nucleus. Considering the nucleus as a gas of nucleons, one could then, for example, apply the statistical theory to such subsequent collisions and predict deuteron-to-proton ratios. Since deuteron production in elementary nucleon-nucleon collisions in the GeV range has recently been measured,[6] one can also utilize these experimentally determined cross sections to estimate the number of deuterons produced by secondary nucleons. The percentage of secondary nucleons giving rise to deuterons should be, according to such an estimate, of the order of magnitude of $R/\lambda$, $R$ being the nuclear radius and $\lambda \approx 1/N\sigma$ the mean free path for deuteron formation, with $N$ being the density of nucleons in the nucleus and $\sigma$ the cross section for deuteron production in an elementary collision. For 2-GeV/$c$ nucleons in aluminum $R/\lambda$ is 0.01, i.e., the order of magnitude of the deuteron-to-proton ratio is correctly predicted. Nevertheless, quantitatively, the experimentally observed deuteron-to-proton ratios are consistently larger than 1%, which suggests some additional enhancement of deuteron production in nuclear matter.

The production of mass-three nuclei is even more difficult to explain if one restricts the production mechanism to elementary nucleon-nucleon interactions. In such interactions tritons should be produced along with antinucleons but there are not enough antinucleons produced altogether to match the large number of tritons unless one assumes an unreasonably large ($\sim$10%) probability of producing tritons along with antinucleons. Moreover, 30° in the laboratory is even further from the kinematical limit for tritons than for deuterons. They would therefore have to be produced by secondary nucleons of much lower energy which have small cross sections for production of antinucleons.

It seems therefore that dense nuclear matter plays an essential part in the formation of deuterons and heavier nuclei. An attractive model of this formation has been proposed by Butler and Pearson.[7] They assume that two shower nucleons coalesce into a deuteron with the nuclear matter acting as a catalyzer. Such a process will be most probable for a low initial relative momentum between the two shower nucleons especially since the deuteron production cross section in elementary nucleon-nucleon collisions has a peak at low relative momenta. Low relative momenta are quite probable within the shower produced in the nucleus by the impinging proton. The reason is twofold. Two shower nucleons which move in the same direction with relativistic velocities have a relative momentum which is smaller than the difference of their momenta as seen from the laboratory. Their relative momentum, which is properly defined as the momentum of one of the nucleons in the rest system of the other, is approximately $(m/E)(k_2-k_1)$ provided $k_2-k_1 \ll E$. Here $m$ is the nucleon rest mass, $k_{1,2}$ are the two laboratory momenta; and $E$ is the laboratory total energy of one of the nucleons. The velocity of light is chosen as unit velocity. On the other had, the transverse momenta of the shower nucleons are small, and, therefore, also the components of their relative momenta perpendicular to the direction of motion of one of them are small.

One may, therefore, attempt to explain the deuteron and triton yield by postulating that they arise from coalescing shower nucleons and explore the consequences of such an assumption. The first condition for its applicability is, of course, that there are sufficiently many shower nucleons. If we extrapolate the empirical formula for the number of secondary protons given above to all angles and assume a 25% target efficiency as well as an equally large neutron yield, we get on the average about three shower nucleons per interacting proton. Deviations from the empirical formula at larger angles do not significantly alter this number.

In the spirit of the two-step model, one may now assume that the deuteron and triton yields are obtained by averaging their respective formation probabilities, which depend on the state of relative motion of the shower nucleons, over all such possible states. Butler and Pearson calculate the deuteron formation probability under the assumption that the nuclear optical potential provides the interaction necessary for the coalescence of shower nucleons. Here, we shall attempt a much more simple-minded approach, by introducing a phenomenological parameter. We assume that any two nucleons whose relative momentum is smaller than a certain momentum $\rho$ coalesce into a deuteron but no others do. Any three nucleons with relative momenta

[6] A. P. Batson, B. B. Culwick, J. G. Hillend, and L. Riddiford, Proc. Roy. Soc. (London) **251**, 218 (1959); G. A. Smith, H. Courant, E. C. Fowler, H. Kraybill, J. Sandweiss, and H. Taft, Phys. Rev. **123**, 2160 (1961); W. J. Fickinger, H. Pickup, D. K. Robinson, and E. O. Salant, *ibid.* **125**, 2082 (1962); B. Sechi Zorn, Bull. Am. Phys. Soc. **7**, 349 (1962).

[7] S. T. Butler and C. A. Pearson, Phys. Rev. Letters **7**, 69 (1961); Phys. Letters **1**, 77 (1962).

within about the same range are supposed to coalesce into a triton or $He^3$, while no others should contribute to their yield. The magnitude of $\rho$ should turn out to be small compared to the laboratory momentum of shower nucleons, if the model is to make sense.

Since the probability of finding any one nucleon within such a small region of momentum space is small, it follows from the above assumptions that the triton-to-deuteron ratio should be of the same order of magnitude as the deuteron-to-proton ratio at any given angle and any given momentum per nucleon. The exact value of this quantity should, of course, depend on a number of parameters such as the probability distribution for different numbers of shower nucleons in the nucleus, statistical weight factors, differences in binding energies, etc. In our experiment we get $d(2\text{GeV}/c)/p(1\text{GeV}/c) \cong t(3\text{GeV}/c)/d(2\text{GeV}/c)$ for the ratios of the yields $dN/dkd\Omega$ of the different particles at the indicated momenta.

The deuteron-to-proton ratio at a given angle $\theta$ and momentum per nucleon $k$ should, according to the above assumptions, be essentially governed by the probability of finding a neutron within a small sphere of radius $\rho$ around the point representing any given proton in momentum space. This probability is, according to expression (1),

$$W(k)=2\times10^{-2}\frac{e^{-[(k\theta)^2/0.7]}}{k\sin\theta}\frac{4\pi\rho^3}{3m}\frac{1}{X}, \tag{2}$$

again assuming that there are as many neutrons as protons among shower nucleons and also that in a shower the number of neutrons is independent of the number of protons. Here $X$ is the target efficiency. The experimentally most directly measured quantity is, however, the ratio of the deuteron yield $dN_d/dKd\Omega$ to the proton yield $dN_p/dKd\Omega$ at the same total momentum $K=2k$, where $k$ is the momentum per nucleon in the deuteron. This quantity is, according to expressions (1) and (2),

$$\frac{dN_d(K)}{dN_p(K)}=\frac{dN_p(k)W(k)}{dN_p(K)}=2\times10^{-2}\frac{e^{[(K\theta)^2/1.4]}}{K\sin\theta}\frac{4\pi\rho^3}{3m}\frac{1}{X}, \tag{3}$$

and is only weakly momentum dependent in the range of our experiments in agreement with the observations. Moreover, it does not violently change with angle, especially if we consider that observations at different angles tended to be made in the same region of transverse momenta. Thus, the approximately constant deuteron-to-proton ratio is correctly predicted. Within this framework, it is also qualitatively understandable that the probability of deuteron formation should increase with nuclear size both owing to the presumably increased average number of shower nucleons per nucleus and the increased length of their path inside nuclear matter.

If we take $X=0.25$, the absolute value of $\rho$ necessary to obtain the experimental deuteron yields equals about 400 MeV/$c$. One could increase the estimated deuteron yields, i.e., decrease $\rho$, by assuming that deuterons arise not only from protons coalescing with neutrons but from any pair of shower nucleons, the nuclear matter taking care of charge conservation. If one neglected any competition from other two-nucleon states of low internal energy, one could, in this way, increase the estimated deuteron-to-proton ratio by at most a factor of 2, thus decreasing $\rho$ to about 300 MeV/$c$. This would, however, constitute a gross overestimate of the deuteron-to-proton ratio, especially since we have already chosen a lower limit for the target efficiency and neglected the unfavorable influence of a finite number of shower nucleons.

It should be possible to justify such a value of $\rho$ by a detailed calculation, since Butler and Pearson were able to fit most experimental data on the deuteron-to-proton ratio surprisingly well. We believe, however, that the large value of $\rho$ makes questionable a quantitative fitting of experimental data to a model which treats nuclear matter as a mere catalyzer in the deuteron formation process. The momentum $\rho$ should, of course, be interpreted as some average relative momentum between two nucleons which have a substantial probability to emerge as a deuteron, and this probability should still be appreciable for pairs of nucleons with a few times larger relative momenta. Nucleons in the tail of the momentum distribution of nuclear matter should thus contribute acceptable partners to at least the slower shower nucleons. One is drawn to the same conclusion also by the large cross section for deuteron production in elementary nucleon-nucleon collisions which was mentioned before.

These considerations indicate that the Butler-Pearson mechanism may well account for a large fraction of deuterons and mass three nuclei produced in high-energy nuclear reactions. On the other hand, the direct contribution of nucleons from the Fermi sea should be reexamined, before one tries to extract quantitative information such as optical-model parameters from a comparison between the Butler-Pearson model and the experimental results.

## ACKNOWLEDGMENTS

We wish to acknowledge the invaluable cooperation of the AGS staff and operating crew. Special thanks are due to Dr. Robert H. Phillips for his constant interest and aid. We are grateful to Dr. M. Goldhaber for several discussions and critical comments.

## APPENDIX

### Electronics

In this Appendix we shall describe some of the special features used to obtain the good time resolution necessary to distinguish particles of quite high momenta with small distance between the counters of the telescope.

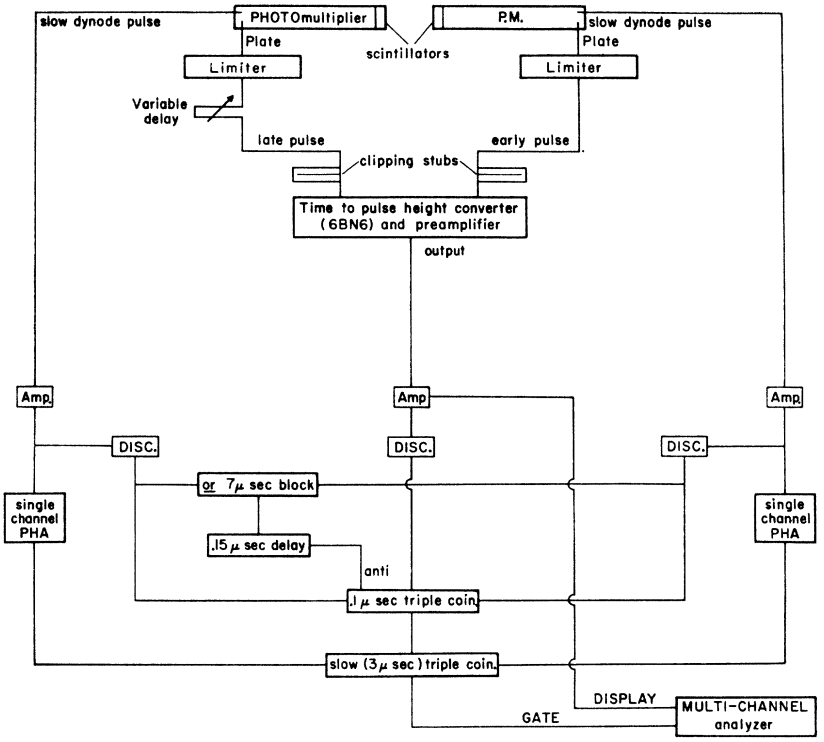


FIG. 10. Schematic diagram of electronics.

A more detailed discussion of the circuitry for time spectroscopy is given elsewhere.[8]

A schematic diagram of the electronics used is given in Fig. 10. This shows the time to amplitude converter, amplitude selecting single-channel pulse-height selectors, and blocking circuitry. It does not show selective storage routing features which are discussed below. All the slow coincidence circuits and single-channel pulse-height selectors are included in a transistorized multiple-coincidence circuit (called M.C.C. below) designed by Chase.[9]

### *A. Block Circuitry*

Blocking circuitry allows the use of relatively slow amplifiers (1-μsec delay line clipped) and slow single-channel analyzers at quite high singles counting rates by removing considerably the effects of pulse pile-up. It also has the effect of improving the time spectra obtained at high rates. In addition it enables determination of dead time losses in the slower circuitry (not the multichannel analyzer) in a simple manner. The block circuitry is shown schematically in Fig. 10. The logical effect is as follows. If a pulse of any amplitude (above noise) appears in *either* photomultiplier, discriminator 1 or 2 fires. These discriminators have an output pulse of 0.1-μsec duration and a recovery time of ~0.1 μsec. After a delay of ~0.15 μsec they produce a blocking signal of 7-μsec duration during which all the succeeding circuitry is turned off. Thus, any pulse produces an artificial dead time of 7 μsec for the analysis of coincidences. One is assured, therefore, that any pulse being analyzed is preceded by a quiet time in both multipliers of at least 7 μsec. This allows complete recovery of all multiplier voltages, limiters, 6BN6 circuit, as well as the recovery of all the slow circuitry. In these experiments the block circuit removed approximately 10% of the coincidences.

The counting of total coincidence pulses, both with and without the block circuitry (performed simultaneously with parallel-coincidence circuitry included in the M.C.C.), leads naturally to the correction for the total system dead time and all our absolute intensity measurements have been so corrected.

### *B. Pulse-Height Selection and Memory Split*

The effects of photoelectron statistics and circuitry rise time upon the width of "time spectra" are well known. These produce apparent shifts in time due to variation of pulse amplitudes.[8] For this reason it has been customary to attempt to restrict the pulse amplitude by a single-channel analyzer and thus to accept only a limited range of pulse heights which are used for time analysis.

For mass spectroscopy by time of flight, restriction of pulse amplitude may seriously affect the relative sensitivity as a function of mass. Each particle has some-

[8] A. Schwarzschild, in *Electromagnetic Lifetimes and Properties of Nuclear States*, Nuclear Science Series Report Number 37 (National Academy of Sciences, National Research Council Publication 974, Washington, D. C., 1962); also Nucl. Instr. Methods (to be published).

[9] R. L. Chase, Rev. Sci. Instr. **31**, 945 (1960).

what different mean ionization in the scintillator as well as varying distributions (Landau distribution) for the different particle. Thus, in principle, one must attempt to accept all pulse amplitudes for the time spectra.

The competing requirements of high efficiency for all types of particles versus restricted pulse amplitude for good time resolution can be overcome with the use of multidimensional pulse-height analyzers. Thus, the time pulse might be stored as a function of pulse amplitude in each detector. Fast multidimensional analyzers were not available at the time of this experiment. However, by employing several single-channel analyzers and multiple coincidence circuitry (M.C.C.) we have been able to use the selective storage features of the RIDL pulse-height analyzer to effectively obtain a two by one-hundred-channel analyzer. As described in Sec. III of this paper, time pulses corresponding to a restricted range of pulse amplitudes in both counters could thus be stored in one section of the analyzer, whereas all pulse pairs not satisfying the limited range of pulse-amplitude selection resulted in storage of the time pulse in the second half of the analyzer memory. The improved time resolution in the restricted amplitude section is clearly seen in Fig. 2. Analysis of these spectra is performed in a straightforward manner by first obtaining the $K^+/\pi^+$ ratio in the solid curve, by inferring the number of unresolved $K^+$ in the opened circle curves, and then adding the total intensities of pions in both spectra and thereby ascertaining the absolute $K^+$ intensity. Without the device of memory split, the resolution of the $K^+$ peak from the $\pi^+$ is subject to much greater background corrections and at higher momenta is essentially impossible.

PHYSICAL REVIEW VOLUME 129, NUMBER 2 15 JANUARY 1963

# Spin Rotation Coefficients in $\pi$-$N$ Scattering

YOUNG S. KIM
*The Ohio State University, Columbus, Ohio*
(Received 27 August 1962)

The spin rotation coefficients of the recoil proton in $\pi$-$N$ scattering are studied from the point of view of providing a means of resolving the present ambiguities in the phase-shift solution of the scattering cross section and the polarization of the recoil proton. There are six possible experiments four of which are independent, and the magnitude and the relative sign of the scattering matrix elements can uniquely be determined by four independent scattering experiments.

## INTRODUCTION

THE advent of partially polarized proton targets[1] opens a new field of possibilities for nuclear experimentalists. Of particular interest to pion physicists is the possibility of measuring the spin rotation coefficients—$A$, $R$, $A'$, and $R'$ (Wolfenstein parameters)—of the recoil proton in $\pi$-$N$ scattering.

It is well known that in the intermediate energy region (from 200 to 400 MeV) several ambiguities still persist in the phase-shift solution of $\pi$-$p$ scattering even with the recently acquired polarization data.[2-4] Even though the present ambiguities can, in principle, be resolved by the polarization experiment,[5-8] due to various experimental difficulties[9] the polarization measurement at present is limited to a small angular region and the "resolving power" of the recoil proton polarization can not be fully utilized. In this paper we discuss several possible experiments which may be used in determining the phase shifts uniquely or in determining the scattering matrix elements.

## DISCUSSIONS

A simple consideration based on the partial-wave analysis shows that a total of $2(2L+1)$ constants[10] are needed to describe each of the ten possible modes of

[1] L. H. Johnston and C. F. Hwang (private communications); W. A. Barker, Revs. Modern Phys. **34**, 173 (1962); L. D. Roberts and J. W. Dabbs, Ann. Rev. Nucl. Sci. **11**, 175 (1961).
[2] E. H. Rogers, O. Chamberlain, J. H. Foote, H. M. Steiner, C. Wiegand, and T. Ypsilantis, Rev. Mod. Phys. **33**, 356 (1961); J. H. Foote, O. Chamberlain, E. H. Rogers, H. M. Steiner, C. Wiegand, and T. Ypsilantis, Phys. Rev. **122**, 948, 959 (1961); E. L. Gregor'ev and N. A. Mitin, J. Exptl. Theoret. Phys. (U.S.S.R.) **37**, 413 (1960) [transaltion: Soviet Phys.—JETP **10**, 295 (1960)].
[3] J. F. Kunze, T. A. Romanowski, J. Ashkin, and A. Burger, Phys. Rev. **117**, 859 (1960).
[4] E. F. Beall, B. Cork, P. G. Murphy, W. A. Wenzel, C. M. P. Johnson, and L. J. Koester, Jr., Phys. Rev. **126**, 1554 (1962).
[5] S. Minami, Progr. Theoret. Phys. (Kyoto) **11**, 213 (1954).
[6] J. Orear, Phys. Rev. **100**, 288 (1955).
[7] J. Deahl, M. Derrick, J. Fetkovich, T. Fields, and G. B. Yodh, Phys. Rev. **124**, 1987 (1961).
[8] E. Fermi, Phys. Rev. **91**, 947 (1953).
[9] The large Coulomb scattering at small angles sets the lower limit and the analyzing power of the $C^{12}$ analyzer which decreases rapidly below 100 MeV sets the upper limit on the angular region in which the polarization can be measured with any reasonable accuracy.
[10] Here $L$ is the largest angular momentum state effecting the scattering. There are $2L+1$ real phase shifts and $2L+1$ amplitudes. For pion energies below 400 MeV the inelastic cross section is small and only the phase shifts need be determined.

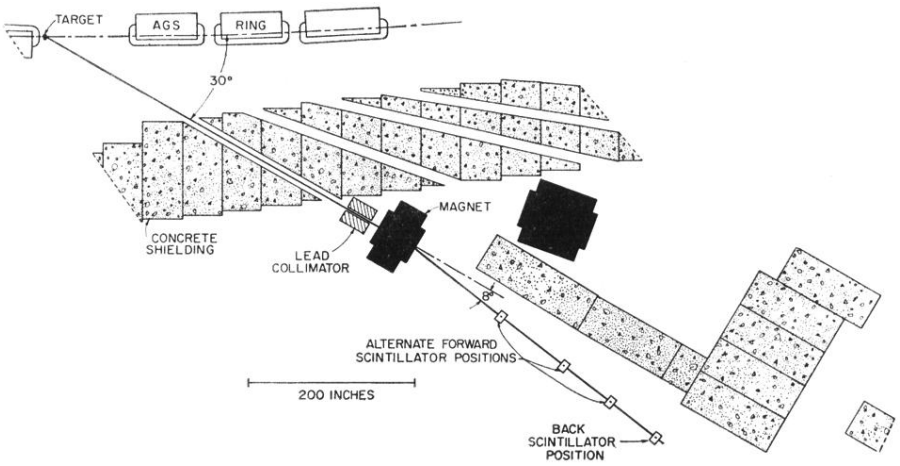


FIG. 1. Experimental arrangement.